Int. J. Advanced Design and Manufacturing Technology, 2024, Vol. 17, No. 4, pp. 11-18

DOI:10.71644/admt.2024.873805 *ISSN: 2252-0406* *https://admt.isfahan.iau.ir*

A Comparative FEM Analysis of a Substituted 3D-Printed U-Joint with PLA and ABS Materials

Mohammad Sajjad Mahdieh *
Department of Mechanical Engineering,
Shahid Chamran University of Ahvaz, Ahvaz, Iran
E-mail: s.mahdieh@scu.ac.ir
*Corresponding author

Golshid Fathinasab
Department of Mechanical Engineering,
Shahid Chamran University of Ahvaz, Ahvaz, Iran
E-mail: golshidfathinasab@yahoo.com

Received: 8 January 2024, Revised: 8 October 2024, Accepted: 2 November 2024

Abstract: Currently, manufacturing and repairing industrial equipment in a short time with the least cost has been a challenge. Furthermore, the idle time of the industrial machines due to their failed parts imposes high losses on the production process. Applying 3D printers to manufacture damaged parts quickly is a promising measure to tackle the abovementioned problem. This article is an efficient approach to the manufacture and analysis of a universal joint (U-joint) as the case study with Polylactic acid (PLA) and Acrylonitrile butadiene styrene (ABS) through the 3D printing process. U-joints are widely used as a coupling in industrial equipment to alleviate the misalignment of input and output shafts in many gearboxes and pumps. Because of undergoing fatigue loads, the failure occurrence in U-joints is very probable. Therefore, an attempt is made here to substitute this part with a 3D-printed one. Besides, comparing and evaluating the results of FEM simulations for the sake of selecting the most suitable material for the U-joint are done. According to the FEM results, the maximum stress imposed on the U-joint was obtained 28.8MPa which is lower than the yield strength of both PLA and ABS materials; however, the results show that PLA has higher fatigue strength than ABS in this case.

Keywords: ABS, 3D-Printing, FEM Analysis, Machine Components, PLA

Biographical notes: Mohammad Sajjad Mahdieh received his PhD in Mechanical Engineering from the University of Tehran, Iran. He is currently an Assistant Professor at the Department of Mechanical Engineering, Shahid Chamran University of Ahvaz, Iran. His research areas are inverse engineering, 3D printing, and metal forming. **Golshid Fathinasab** is a graduate of the Department of Mechanical Engineering, Shahid Chamran University of Ahvaz, Iran.

Research paper

1 INTRODUCTION

A universal joint is a connection between two shafts, typically yokes, that enables relative rotation around the y and z axes. This joint includes input and output shafts and an intermediate cross pin. Meaning that the input shaft is capable of transferring torque and rotary motion by means of cross to the output shaft. It is possible that rotation to be conveyed between the shafts while allowing misalignment in both axes. Car manufacturing, excavation, and robotics are examples of applications in which universal joints have been used. This explains why have been decided to consider it in a specific situation [1]. To manufacture most of the mechanical parts, applying finishing processes such as grinding, vibratory finishing, burnishing, and barrel finishing is inevitable [2-6]. Figure 1 shows the U-joint as the case study and its dimensions. 3D printing through quick and easy methods makes the production process more optimized and faster, thereby economizing on expenditures and time. Failing industrial parts not only causes excessive damage but also stops machines.

3D printers have solved these problems by constructing plastic components that have approximately similar properties to metal ones and can even temporarily work. There are some examples of profitable and practical consequences of using 3D printing. Cwekla et al. in 2017, studied mechanical strength properties of 3D-printed elements. Their research was carried out on a set of standardized samples, printed with low-cost standard materials (ABS), using a cheap 3D printer. The influence of parameters (such as the type of infill pattern, infill density, shell thickness, printing temperature, and the type of material) on selected mechanical properties of the samples, was tested [7].

In 2020, Kiendl et al. checked out the mechanical properties, especially toughness, strength, and stiffness, of FDM 3D-printed cases made of PLA. It was discovered that the material was isotropic in terms of stiffness and strength, but not at all in terms of toughness. furthermore, the material demonstrated much higher toughness when loaded cornerwise in comparison with loading parallel/perpendicular to the raster. It is possible to acquire optimized material performance purveying not only high strength but also high toughness simultaneously [8]. Goyanes et al. investigated the feasibility of using fused deposition modeling (FDM) with Hot Melt Extrusion (HME) and fluid bed coating to fabricate modified-release budesonide dosage forms [9]. Popa et al. in 2023, studied the experimental and numerical analyses of the impact parameters. They comprehended that materials made by additive manufacturing are able to be numerically modeled and calibrated with experimental ones. This means that the kinetic energies achieved in the numerical analysis of the PLA material had resemblance values to the experimental one [10]. FEM simulation helps to reduce the probable errors in manufacturing and the total cost [11-13].

Rarani et al. produced an industrial part with two different polymers: pure polylactic (PLA) and carbon fiber-reinforced PLA. Then they assessed the mechanical properties of the 3D printed samples through experiments such as tensile test and 3-point bending [14]. In addition, Akhoundi et al. investigated the effect of the filling pattern on tensile and flexural strength and modulus of the parts printed via fused deposition modeling (FDM), 3D printer [15]. Moreover, Vijayaraghavan et al. proposed an improved approach of multi-gene genetic programming (Im-MGGP) to formulate the functional relationship between wear strength and input process variables of the FDM process [16].

Deswal et al. in 2019, optimized significant process parameters including layer thickness, build orientation, infill density, and the number of contours for enhancing the magnitude/dimensional preciseness of fused deposition modeling (FDM) devise units [17]. San Andrés et al. probed about using 3D printing PLA and ABS materials for fine art. Samples were arranged in two diverse shapes (filament and printed parts). ABS showed noticeable changes against both sources of exposure (UV radiation and temperature), especially after UV aging, but PLA experienced more changes through temperature aging than UV radiation. This means that PLA generally demonstrated better stability than ABS [18].

In 2023, Karami Moghadam et al. studied how the CO2 laser cutting and Fused Filament Fabrication (FFF) 3D printing parameters influence the surface morphology of PLA samples. As a result of this article, through this way, not only the surface roughness of FFF parts was well diminished but also created a uniform surface texture [19]. In 2022, Martin et al. evaluated polymer composite based on PLA, elastomers, and cellulosic fibers through direct extrusion of crude materials in the pellet form for 3D printing. In general, these mentioned polymer composites were recognized as the most appropriate for pellet-based extrusion 3D printing [20]. It is worth mentioning that the 3D-printed parts may require machining processes to obtain the desired surface quality [21-27].

In this paper, a comparative analysis of a 3D-printed universal joint with PLA and ABS materials is accomplished. The industrial U-joint used as the case study in this project is shown in “Fig. 1”. This U-joint is applied to connect the small motor to the gearbox in a small drilling machine and this study attempts to substitute it with a 3D-printed one. Designing and simulation are done through SolidWorks software and Ansys Workbench software respectively. The most acceptable material of joint for use as a coupling in

industrial equipment in terms of life, safety factor, stress, and deformation should be concluded at the end. In addition, the U-joint is 3D printed by an FDM machine, and its function is investigated experimentally.

Fig. 1 Industrial U-joint as the case study.

2 MATERIALS AND METHODS

In this study, the feasibility of substituting a U-joint of an industrial machine's coupling with a plastic 3D-printed U-joint is investigated via FEM simulation. In this case, in order to calculate the functional life of the 3D-printed U-joint while applying in the coupling, the maximum bending stress, contact stress, and maximum strains are obtained through simulation by Ansys software. The specifications of the mentioned U-joint, the properties of the polymer used in the FDM machine, and the parameters adjusted in U-joint software are explained in the following.

2.1. Specifications of the U-Joint

In the first place, the universal joint was designed through SolidWorks software 2020. Designing includes two divisions, part, and assembly which are used for a 3D representation of a single design component and a 3D arrangement of parts or other assemblies respectively. Universal joints contain two driven yokes and a spider. In "Fig. 2" the 3D model of the U-joint performed in SolidWorks software is illustrated.

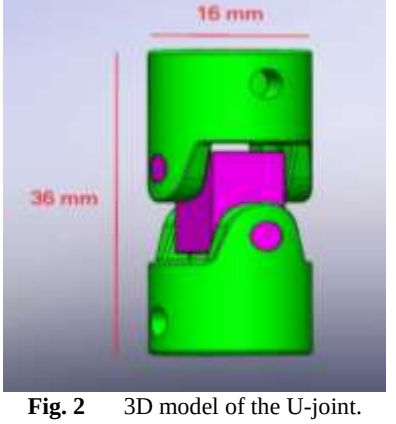

Fig. 2 3D model of the U-joint.

2.2. Properties of Materials and 3d Printing Machine

In this project, two polymers ABS and PLA which are very common for this purpose, are applied. The Mechanical properties of PLA and ABS filament used in the Property module of Ansys are presented in "Table 1".

Table 1 Mechanical properties of ABS and PLA

Properties	ABS	PLA
Elongation at Break	10 - 50 %	41.3 - 63.8%
Elongation at Yield	1.7 - 6 %	2.00%
Flexibility (Flexural Modulus)	1.6 - 2.4 GPa	3,280 MPa
Hardness Shore D	100	66
Stiffness (Flexural Modulus)	1.6 - 2.4 GPa	4.2 GPa
Strength at Break (Tensile)	29.8 - 43 MPa	38 - 47.8 MPa
Strength at Yield (Tensile)	29.6 - 48 MPa	37-46 MPa
Young Modulus	1.79 - 3.2 GPa	4.8 GPa

The model of the 3D printer applied in this present project is Ender-3 v2 neo of the Creality Company. The diameter of its nozzle is 0.4mm and the filament's feed rate is 50 mm/s. In addition, the diameter of the filament is 1.75mm. Figure 3 shows the 3D printer and filaments.

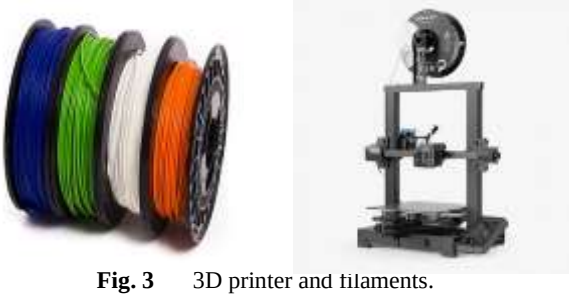

Fig. 3 3D printer and filaments.

Simulation Parameters

To analyze this problem in Ansys, three modules can be used: rigid dynamic, static structural, and transient structural. In the present study, the third module-transient structural- has been applied. The transient structural module is proper for problems with high deflection as well as high velocity. This module also has a higher analysis rate.

In the next step, connections among parts in the Connection module were defined. In the other world, the boundary conditions were set. In the Contact module, the action and reaction of parts when colliding with each other are defined. In this section, if no contact is defined between two parts, these two parts pass through each other. Therefore, three kinds of contacts can be defined among parts: frictional, sticking, and no frictional. In the

present project, the frictional contact was defined. Figure 4 shows the boundary conditions among parts. These constraints were defined as the movement and rotation of the U-joint being in harmony with the real one. The coefficient of friction was set equal to 0.2. The distributed torque was imposed to the one-half of the coupling equal to 1N.m. The value of this torque was obtained by calculating the output power of the gearbox and rotational speed.

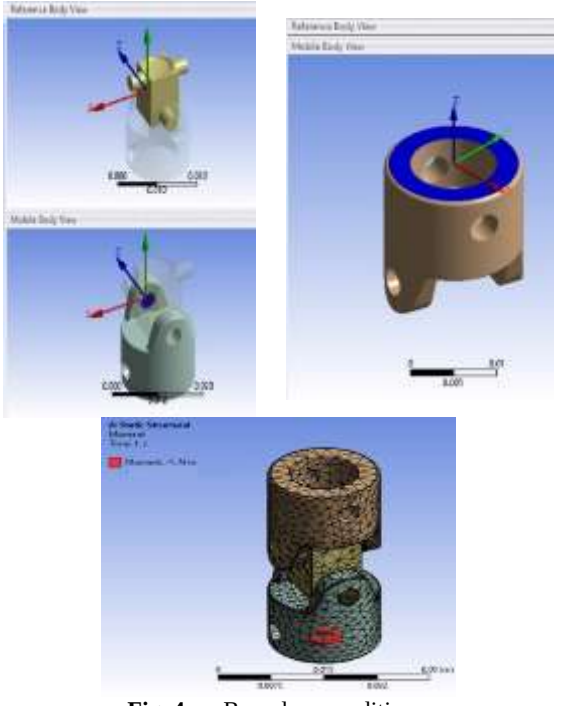

Fig. 4 Boundary conditions.

The Meshing is defined in the Mesh module. According to "Fig. 5", meshing was performed between the parts. Here, due to the significance of the pins of the connecting part and the holes of the coupling halves, these sections have fine mesh sizes; despite the other parts which have larger mesh sizes.

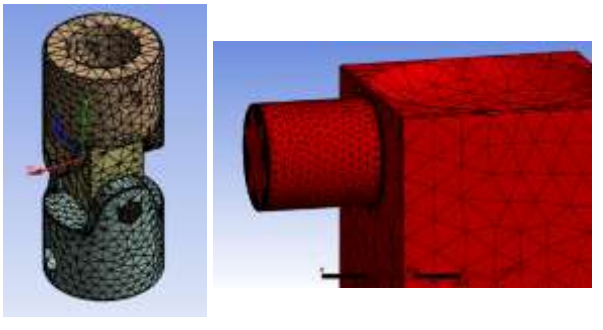

Fig. 5 Meshed parts.

If the mesh size of the whole of the mechanism is identical, the run time increases dramatically. The mesh size is 2mm and it is a 2D (surface mesh) type. In addition, the mesh control was applied to investigate the convergence of the results.

3 RESULTS AND DISCUSSIONS

In this entry, the feasibility of substituting a U-joint of an industrial machine's coupling with a plastic 3D-printed U-joint is investigated via FEM simulation. In this case, in order to calculate the functional life of the 3D-printed U-joint while applying the coupling, the maximum bending stress, contact stress, and maximum strains are obtained through FEM simulation by ANSYS software as follows.

3.1. Static Analysis

The first step involves evaluating the points that exhibit the highest stress levels. The values obtained for the stresses at these points must be compared to manually calculated results for validation purposes. By comparing these two sets of results and minimizing the error, the accuracy of the simulation is confirmed. Therefore, the most suitable material for constructing this universal joint can be determined by comparing the FEM results of two materials, ABS and PLA.

According to "Fig. 6", by imposing the torque to one-half of the coupling, the maximum stress was obtained and it is equal to 28.8MPa which is lower than the yield strength of both PLA and ABS materials. As it is obvious, the critical points are located at the spider part (on its pins). In reality, the same phenomenon occurs and most similar U-joints are damaged by their spiders.

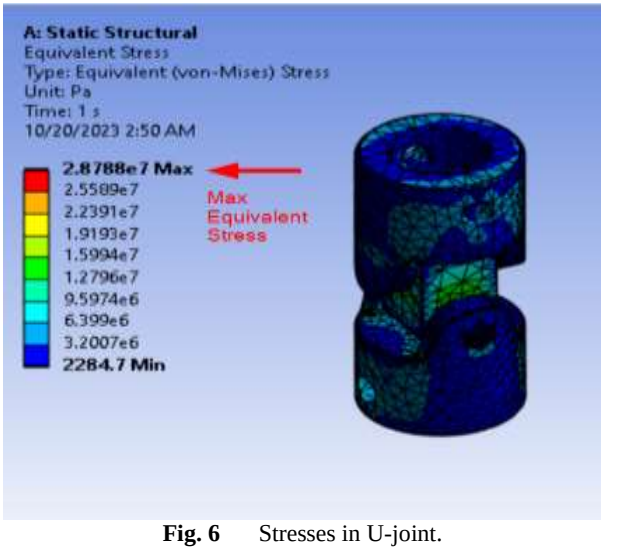

Fig. 6 Stresses in U-joint.

In this section, the manual analysis of the universal joint is presented. First, we manually calculated shear stress and bearing stress for the spider. Then, we identified the elements with the maximum stress values compared to

the calculated values. It was noteworthy that the obtained number for bearing stress is related to an element on the pin's surface, and the shear stress is calculated on the pin's cross-section. Finally, we determined the percentage of error between theoretical and software-generated values. The maximum bearing stress and shear stress on the spider's pin are manually calculated as follows.

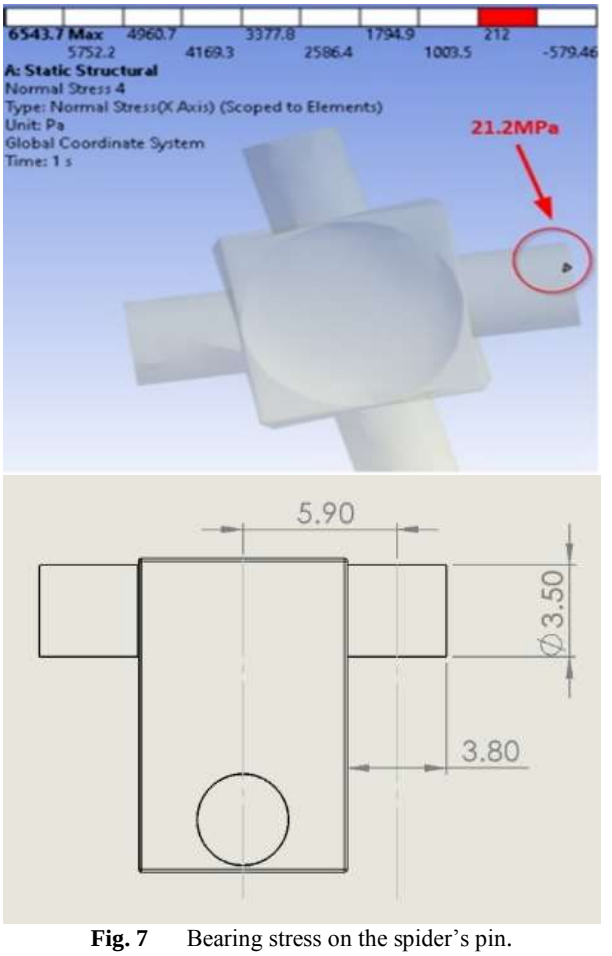

Fig. 7 Bearing stress on the spider's pin.

As following the equations, the bearing stress on the spider's pin was calculated at approximately 22.8 MPa. On the other hand, according to "Fig. 7", the maximum normal stress obtained by FEM analysis was 21.2MPa which indicates a 4.4% error.

$$T = 1NM$$

$$F = \frac{T}{2} \times r$$

$$\text{Bearing stress } \sigma = \frac{F}{A} = 22.8Mpa$$

$$\text{Error percentage: } \frac{22.8-21.2}{22.8} \times 100 \approx 4.42\%$$

The shear stress in the spider's pin has the same story. The manually calculated shear stress was equal to 20.9 MPa versus 21.2MPa obtained through FEM simulation ("Fig. 8") with a 1.5% error.

Then, to manually analyze the normal stress imposed on the corner of the half-coupling due to the bending phenomenon, this section was modeled with a cantilever beam as shown in "Fig. 9". Consequently, the maximum normal stress at the critical point was calculated at about 22.2MPa which is lower than the yield strength of the materials.

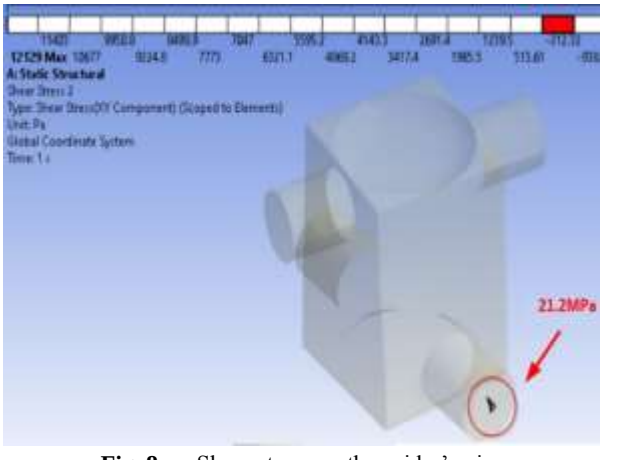

Fig. 8 Shear stress on the spider's pin.

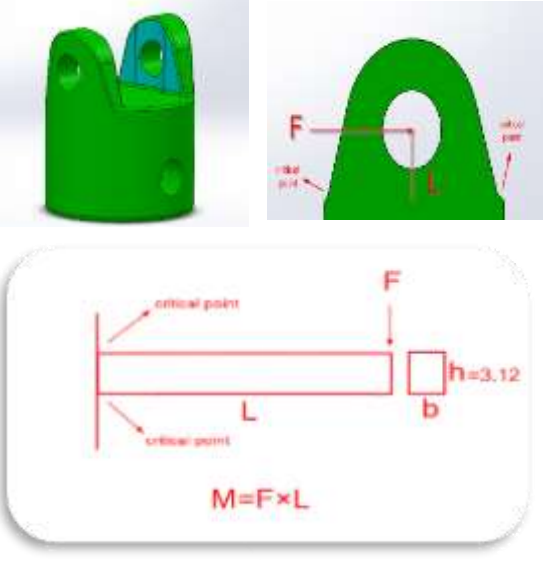

Fig. 9 Modelling of half-coupling with a cantilever beam.

3.2. Life Analysis

In this section, the lives of both materials (ABS & PLA) through fatigue analysis in static structural modules are determined and compared. The maximum stress is endured by spider. In fatigue analysis, where the piece gets damaged is investigated and the duration of this

process for both materials is obtained so that one can choose the best material for construction.
To calculate the life through the fatigue tool section, as shown in "Fig. 10", the loading type was supposed fully reversed with 1.1 as the scale factor and Soderberg as the mean stress theory.

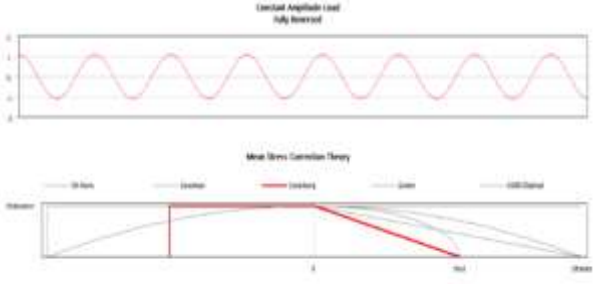

Fig. 10 Set parameters for life analysis.

Figure 11 shows the result of the life analysis for ABS material. As it is obvious, the critical elements (on the root of the spider's pin) endured about 2.67 million cycles. While, these elements in PLA material, endured 3.2 million cycles which indicates the higher fatigue strength of PLA.

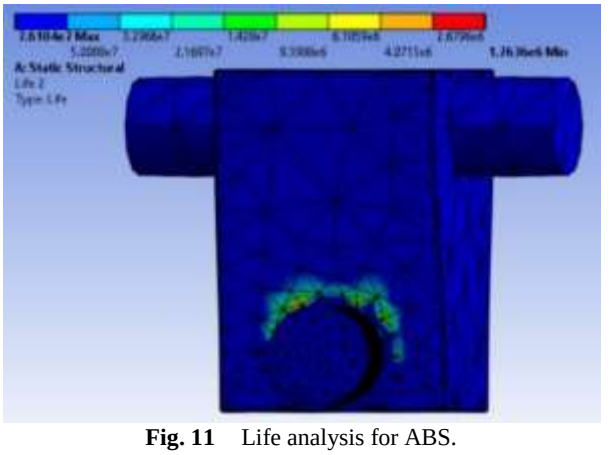

Fig. 11 Life analysis for ABS.

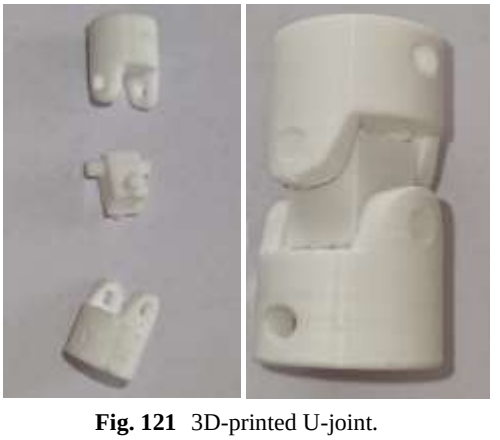

Fig. 121 3D-printed U-joint.

It is worth mentioning that the U-joint was manufactured through the 3D printer machine (demonstrated in "Fig. 12") and applied in the related mechanism. In addition, it has been working thoroughly and correctly without any failure within two months.

4 CONCLUSIONS

In this paper, a comparative analysis of a 3D-printed universal joint with PLA and ABS materials was accomplished. Designing and simulation were done through SolidWorks and Ansys Workbench software respectively. The FEM results were compared with analytical results, moreover, the endurance of the materials was investigated as well. The summary of the results is as follows:

- By imposing the torque to one-half of the coupling, the maximum stress was obtained 28.8MPa which is lower than the yield strength of both PLA and ABS materials.
- The bearing stress on the spider's pin was manually calculated at 22.8 MPa which has a 4.4% error with the FEM results.
- The manually calculated shear stress was equal to 20.9 MPa versus 21.2MPa obtained through FEM simulation with 1.5% error.
- The maximum normal stress at the critical point of the half-coupling was manually calculated at about 22.2MPa which is lower than the yield strength of the materials.
- The critical elements (on the root of the spider's pin) endured about 2.67 million cycles. While, these elements in PLA material, endured 3.2 million cycles which indicates the higher fatigue strength of PLA.

ACKNOWLEDGMENTS

We are grateful to the Research Council of Shahid Chamran University of Ahvaz for financial support (SCU.EM1403.39184).

REFERENCES

[1] Kohli, A., et al., Analysis of Universal Joint Using Virtual Simulation Method, Materials Today: Proceedings, Vol. 59, 2022, pp. 858-866.

[2] Mahdieh, M. S., Rafati, E., and Kargar Sichani, S., Investigation of Variance of Roller Burnishing Parameters on Surface Quality by Taguchi Approach. ADMT Journal, Vol. 6, No. 3, 2013.

[3] Saraeian, P., et al., Influence of Vibratory Finishing Process by Incorporating Abrasive Ceramics and Glassy Materials on Surface Roughness of CK45 Steel. ADMT Journal, Vol. 9, No. 4, 2016, pp. 1-6.

[4] Vakili Sohrforozani, A., et al., A Study of Abrasive Media Effect on Deburring in Barrel Finishing Process. Journal of Modern Processes in Manufacturing and Production, Vol. 8, No. 3, 2019, pp. 27-39.

[5] Vakili Sohrforozani, A., et al., Effects of Abrasive Media on Surface Roughness in Barrel Finishing Process. ADMT Journal, Vol. 13, No. 3, 2020, pp. 75-82.

[6] Mahdieh, M. S., Zadeh, H. M. B., and Reisabadi, A. Z., Improving Surface Roughness in Barrel Finishing Process Using Supervised Machine Learning, Journal of Simulation and Analysis of Novel Technologies in Mechanical Engineering, Vol. 15, No. 2, 2023, pp. 5-15.

[7] Ćwikła, G., et al. The Influence of Printing Parameters on Selected Mechanical Properties of FDM/FFF 3D-Printed Parts, In IOP Conference Series: Materials Science and Engineering, IOP Publishing, 2017.

[8] Kiendl, J., Gao, C., Controlling Toughness and Strength of FDM 3D-Printed PLA Components Through the Raster Layup, Composites Part B: Engineering, 2020, Vol. 180, pp. 107562.

[9] Goyanes, A., et al., Fabrication of Controlled-Release Budesonide Tablets via Desktop (FDM) 3D Printing, International Journal of Pharmaceutics, Vol. 496, No. 2, 2015, pp. 414-420.

[10] Popa, C. F., et al., Numerical and Experimental Study for FDM Printed Specimens from PLA under IZOD Impact Tests, Materials Today: Proceedings, Vol. 78, 2023, pp. 326-330.

[11] Mahdieh, M. S., Esteki, M. R., Feasibility Investigation of Hydroforming of Dental Drill Body by FEM Simulation. Journal of Modern Processes in Manufacturing and Production, Vol. 11, No. 2, 2022, pp. 71-83.

[12] Mahdieh, M. S., Monjezi, A., Investigation of an Innovative Cleaning Method for the Vertical Oil Storage Tank by FEM Simulation, Iranian Journal of Materials Forming, 2022.

[13] Mahdieh, M. S., et al., A Study on Stamping of Airliner's Tail Connector Part through FEM Simulation, Journal of Simulation and Analysis of Novel Technologies in Mechanical Engineering, 2023.

[14] Heidari-Rarani, M., Rafiee-Afarani, M., and Zahedi, A., Mechanical Characterization of FDM 3D Printing of Continuous Carbon Fiber Reinforced PLA Composites, Composites Part B: Engineering, Vol. 175, 2019, pp. 107147.

[15] Akhoundi, B., Behravesh, A. H., Effect of Filling Pattern on The Tensile and Flexural Mechanical Properties of FDM 3D Printed Products, Experimental Mechanics, Vol. 59, No. 6, 2019, pp. 883-897.

[16] Vijayaraghavan, V., et al., Process Characterisation of 3D-Printed FDM Components Using Improved Evolutionary Computational Approach, The International Journal of Advanced Manufacturing Technology, Vol. 78, No. 5, 2015, pp. 781-793.

[17] Deswal, S., Narang, R., and Chhabra, D., Modeling and Parametric Optimization of FDM 3D Printing Process Using Hybrid Techniques for Enhancing Dimensional Preciseness, International Journal on Interactive Design and Manufacturing (IJIDeM), Vol. 13, No. 3, 2019, pp. 1197-1214.

[18] San Andrés, M., et al., Use of 3D Printing PLA and ABS Materials for Fine Art, Analysis of Composition and Long-Term Behaviour of Raw Filament and Printed Parts, Journal of Cultural Heritage, Vol. 59, 2023, pp. 181-189.

[19] Karamimoghadam, M., et al., Influence of Post-Processing CO2 Laser Cutting and FFF 3D Printing Parameters on The Surface Morphology of PLAs: Statistical Modelling and RSM Optimisation, International Journal of Lightweight Materials and Manufacture, Vol. 6, No. 2, 2023, pp. 285-295.

[20] Martin, V., et al., Low-cost 3D Printing of Metals Using Filled Polymer Pellets, HardwareX, Vol. 11, 2022, pp. e00292.

[21] Mahdieh, M. S., The Surface Integrity of Ultra-Fine Grain Steel, Electrical Discharge Machined Using Iso-Pulse and Resistance–Capacitance-Type Generator. Proceedings of the Institution of Mechanical Engineers, Part L: Journal of Materials: Design and Applications, Vol. 234, No. 4, 2020, pp. 564-573.

[22] Mahdieh, M. S., Recast Layer and Heat-Affected Zone Structure of Ultra-Fined Grained Low-Carbon Steel Machined by Electrical Discharge Machining. Proceedings of the Institution of Mechanical Engineers, Part B: Journal of Engineering Manufacture, Vol. 234, No. 5, 2020, pp. 933-944.

[23] Mahdieh, M. S., Mahdavinejad, R., Comparative Study on Electrical Discharge Machining of Ultrafine-Grain Al, Cu, and Steel, Metallurgical and Materials Transactions A, Vol. 74, No. 12, 2016, pp. 6237-6247.

[24] Mahdieh, M. S., Zare-Reisabadi, S., Effects of Electro-Discharge Machining Process on Ultra-Fined Grain Copper, Proceedings of the Institution of Mechanical Engineers, Part C: Journal of Mechanical Engineering Science, Vol. 233, No. 15, 2019, pp. 5341-5349.

[25] Mahdieh, M. S., Mahdavinejad, R. A., A Study of Stored Energy in Ultra-Fined Grained Aluminum Machined by Electrical Discharge Machining. Proceedings of the Institution of Mechanical Engineers, Part C: Journal of Mechanical Engineering Science, Vol. 231, No. 23, 2017, pp. 4470-4478.

[26] Mahdieh, M. S., Mahdavinejad, R., Recast Layer and Micro-Cracks in Electrical Discharge Machining of Ultra-Fine-Grained Aluminum. Proceedings of the Institution of Mechanical Engineers, Part B: Journal of Engineering Manufacture, Vol. 232, No. 3, 2018, pp. 428-437.

[27] Mahdieh, M. S., Improving Surface Integrity of Electrical Discharge Machined Ultra-Fined Grain Al-2017 by Applying RC-Type Generator, Proceedings of

the Institution of Mechanical Engineers, Part E: Journal of Process Mechanical Engineering, 2023, pp. 09544089231202329.